DETAILED STUDY OF A LATERAL SPREADING FOLLOWING THE 2020 PETRINJA EARTHQUAKE (M_W = 6.4) - KUPA RIVER (CROATIA)

NGUYEN LAURA [1], MOIRIAT DENIS [1], GÉLIS CÉLINE [1], HÜRTGEN JOCHEN [2], BENZ-NAVARETTE MIGUEL [3], MRAVLJA BRUNO [4], LUONG TUAN ANH [3], REIFFSTECK PHILIPPE [5], JOSEPHINE LOUIS KIM [2], BAIZE STEPHANE [1], BELIĆ NIKOLA [6], MASLAČ JOSIPA [6], WACHA LARA [6], KORDIĆ BRANKO [6] AND MARKUŠIĆ SNJEŽANA [4]

[1] IRSN, France, *laura.nguyen@irsn.fr*; *denis.moiriat@irsn.fr*; *céline.gelis@irsn.fr*; *stephane.baize@irsn.fr*

[2] RWTH Aachen University, Germany, *j.huertgen@nug.rwth-aachen.de*; *kim.josephine.louis@rwth-aachen.de*

[3] Sol Solution, France, *mbenz@sol-solution.com*; *taluong@sol-solution.com*

[4] University of Zagreb, Faculty of Science, Croatia, *bruno.mravlja@gfz.hr; markusic@gfz.hr*

[5] Gustave Eiffel University, France, *philippe.reiffsteck@univ-eiffel.fr*

[6] HGI-CGS, Croatia, *nbelic@hgi-cgs.hr*; *jmaslac@hgi-cgs.hr*; *lwacha@hgi-cgs.hr*, *bkordic@hgi-cgs.hr*

Introduction

The Petrinja earthquake in Dec. 2020 caused extensive liquefaction occurrences with a lot of sand blows and cracks in the alluvial plain of the Kupa river and, in some of its meanders, local ground subsidence and lateral spreading. All these features are located in flat areas close to the riverbanks in the youngest alluvial terrace (Holocene). From the ground surface, these sediments correspond to 2 m thick clayey silts (Unit 1) overlying different sands at least 3 m thick (Unit 2) and then gravels (Unit 3). Hydraulically, Units 2 and 3 are water-saturated by the alluvial aquifer of the Kupa. All the sand blows correspond to poorly graded sands with silts (SP-SM or SM) and originate from sand bars developped in the convex parts of meanders and buried between 3 and 6 m below the surface (Luong et al., 2023).

This work focuses on one convex meander whose sedimentary aggradation geometries are well highlighted by the DEM image with 0.5 m resolution (points bars, Fig. 1A). Its southern part (site D1) presents alignments of sand blows still observable in 2022, while its northern part (site D2) shows a distribution of long open fissures up to more than 90 m from the bank, reflecting a lateral movement towards the river channel. Only a few traces of sand blows can still be seen on D2 site in 2022.

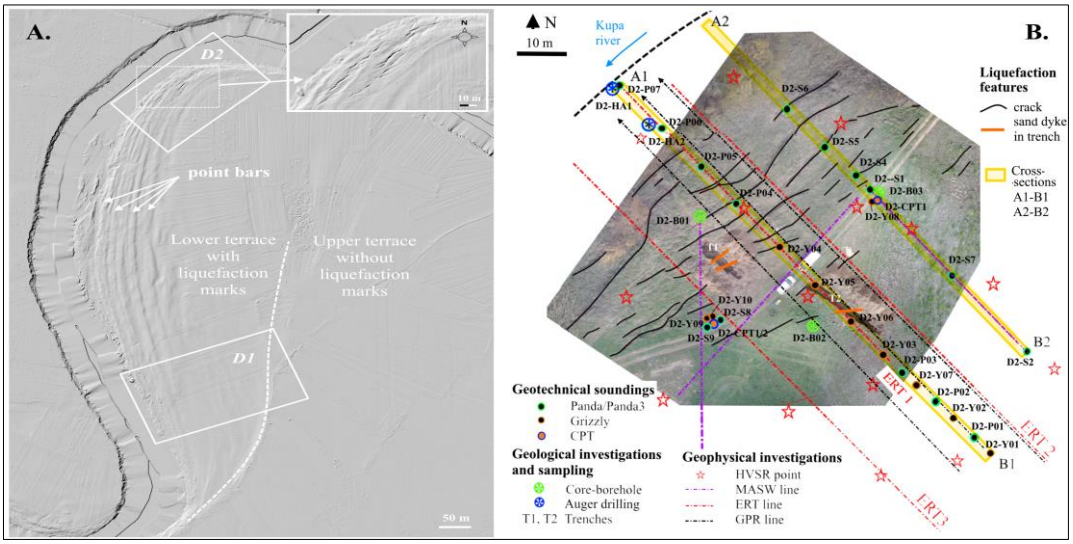

Figure 1. A. Digital Elevation Model (DEM) of site D and B. Location of investigations at site D2

This sliding of non-liquefable layers over liquefied material at depth depends on many factors including the thickness and depth of the liquefied layer (Bunn & Gillins, 2015). In order to identify the causes and mechanisms of this lateral spreading, geotechnical and geophysical investigations were carried out at sites D1 and D2 between Sept. 2022 and March 2024 (Fig. 1B).

Methods

Given the geological context, the guiding idea was to intersect the structures by carrying out cross-sections perpendicular to the Kupa riverbanks (Fig. 1B). We prospected up to a depth of 15 m which is the maximum depth known for surface liquefaction occurrence (Huang & Yu, 2013). Geophysical measurements such as Ambient noise measurements (HVSR), Multichannel Analysis of Surface Waves (MASW), Ground Penetrating Radar (GPR) and Electric Resistivity profiles (ERT) were carried out notably to highlight the geometries of structures at depth. They supplement geotechnical soundings (Dynamic Cone Penetrometer Tests DCPT) and core-boreholes in order to build a detailed model of this lateral spreading. Four trenches for observations and sampling and shear vane tests in cohesive soils also allow to underline the differences between D1 and D2 sites. The results of three Cone Penetrometer Testing (CPT) implemented in 2024 (Fig. 1B) have not yet included in the analysis.

Results

Whatever D1 or D2 sites, the limits at depth between the sedimentary units (Units 1 to 3) show large undulations along a cross-section (Fig. 2) with the same wavelength as those of the points bars at the surface (Fig. 1A). However, this sedimentary organisation in sub-horizontal layers is disturbed locally by subvertical rises of liquefied materials within the Units 1 and 2 (clearly identified on ERT profiles). Above sand blows or sand dykes in trenches, the HVSR measurements reveal a high frequency peak between 4 and 6 Hz. The combination with the Vs measurements (MASW) between 100 and 150 m/s in Unit 1 and 2 (Fig. 2) tends to pinpoint a strong contrast at the bottom of Unit 2 and presumably due to liquefaction of the layers overlying this contrast.

Unlike D1, the site D2 would have presented during the ground shaking a continuous and thicker liquefied layer in the Unit 2 (Fig. 2) allowing lateral movement of non-liquefiable layers above it. All the sandy materials in this liquefied layer are prone to liquefaction with grain sizes close to those of sand blows or sand dykes sampled in the trenches. Their soil resistance (q_d < 2 MPa) and their low shear wave velocity (Vs < 150 m/s) also correspond to loose to very loose sediments. Moreover, the undrained cohesion of the silty cover of Unit 1 at site D2 (~75 KPa) lower than that measured at the site D1 (~125 KPa) must have facilitated fracturing as a result.

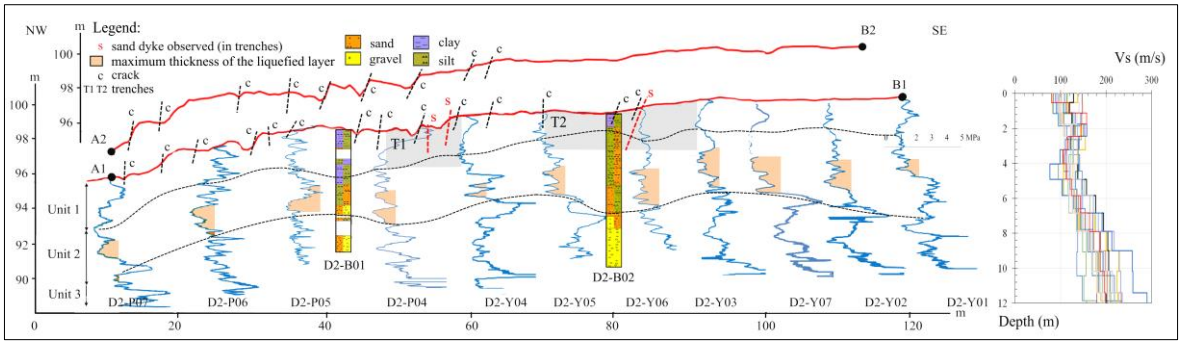

Figure 2. Site D2 - Geotechnical cross-section of a lateral spreading (location on Fig. 1B)

Conclusion

This work sets out the conditions that led to the occurrence of a lateral spreading (site D2) during the Petrinja earthquake in a convex part of a meander of the Kupa river and underlines the notable differences with an adjacent area with only alignments of sand blows at its surface (site D1).

References

Bunn, M.D. and Gillins, D.T., 2015. Assessing lateral spread analysis in areas prone to great and long-duration earthquakes." USGS Report Award G14AP00067.

Huang, Y. and Yu, M., 2013. Review of soil liquefaction characteristics during major earthquakes of the 21st century, Natural Hazards, 65(3): 2375-2384.

Luong, T.A. et al. 2023. Use of the new dynamic cone penetrometer for the study of soil liquefaction along the Kupa (Croatia), Proceedings of the 9th Conf. Croatian Geotech., May 4- 6., ISBN: 978-953-48525-2-1, 101-110.

MACROSEISMIC DATA TO CHARACTERIZE LOCALIZED TOPOGRAPHICAL DAMAGE PATTERNS IN NORTHERN CROATIA AFTER 2020 ZAGREB AND PETRINJA EARTHQUAKES

DAVOR STANKO [1], IVICA SOVIĆ [2], SNJEŽANA MARKUŠIĆ [2]

[1] University of Zagreb, Faculty of Geotechnical Engineering, Varaždin, Croatia; *davor.stanko@gfv.hr*

[2] University of Zagreb, Faculty of Science, Department of Geophysics, Zagreb, Croatia, *sovic@gfz.hr*; *markusic@gfz.hr*

Introduction

On 22 March 2020, Zagreb was hit by the strongest earthquake since 1880 with a magnitude of 5.5 (Markušić et al. 2020). The intensity of VII-VIII °EMS-98 was observed near the epicentral area. In the same year, on 29 December 2020, the wider Petrinja area was hit by a destructive earthquake of magnitude 6.2 with an observed intensity of VIII °EMS (Markušić et al. 2021) in the epicentral area (Figure 1). A considerable part of the reported damage (intensity VI according to EMS classification) to churches, museums, cultural and older buildings and houses in Northern Croatia occurred in topographical areas (marked in Figure 1).

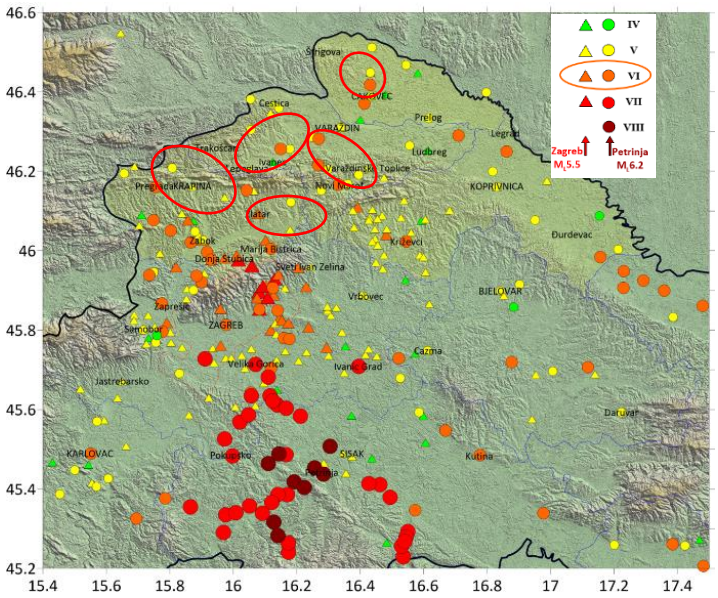

Figure 1. Macroseismic data from 2020 Zagreb and Petrinja earthquakes. (Source of data: Ivica Sović, Seismological Survey of Croatia at University of Zagreb, Faculty of Science, Department of Geophysics)

Methods

Relevant macroseismic observations and data for the study region are compiled from the most recent events of 2020. Macroseismic data (archives, church records) from historical earthquakes in this region, i.e., Međimurje M5.1 in 1738, Great Zagreb M6.3 in 1880, Mt. Ivanščica M4.7 in 1982, Kraljev Vrh M4.9 in 1990 and Ludbreg-Kalnik M4.7 in 1993 are also collected to analyze possible differences between stratigraphic and topographic macroseismic intensity observations and the associated impact on damage.

Results

Table 1. shows the macroseismic observations of the most recent events of 2020 in Northern Croatia with a classification of damage according to the EMS98 scale. For example, in Trakošćan Castle, which was built on a topographic peak, slight damage was observed in the form of diverging thin cracks that formed in places that are important for the load-bearing capacity of the masonry vaults (Markušić et al. 2021b). The first damage to the Chapel of St. Margarete in Kapelščak was also detected in March 2020,

and new damage with internal and external cracks appeared after December 2020. The Diocese of Varaždin has closed numerous churches that were damaged in those two earthquakes. It is worth mentioning that several places (e.g., Trakošćan, Klenovnik, Kraljev Vrh, Koprivnički Bregi, Ludbreg, Kalnik, Novi Marof, Krapina) were also damaged by relatively moderate earthquakes in 1982, 1990 and 1993. Historical earthquakes provide a deep insight into the consequences, and new findings from recent events are helpful in mitigating the consequences of future earthquakes, especially in topographic areas.

Table 1. Some topographic locations with reported damage from earthquakes in 2020 with damage classification according to the EMS98 scale (based on data provided by the Conservation Departments of Varaždin and Krapina)

County	Site / Object	EMS98 damage 2020 earthquakes	Historical earthquake damage
Međimurje	Kapelščak - Chapel of St. Margarete	K2	1738
	Štrigova - Church of St. Jerome	K2	1738, 1880
Varaždin	Klenovnik Castle (Hospital)	K2	1982
	Maruševec - Church of St. George	K3	1982
	Trakošćan Castle	K2	1880, 1982
	Natkrižovljan – Church of St. Barbara	K2	1880
Koprivnica-Križevci	Novi Marof – Castle Erdody (Hospital)	K2	1880, 1982, 1993
	Koprivnički Bregi – Church of St. Rok	K2	1993
	Gornji Dubovec - Church of St. Margaret	K3	1993
	Laz Bistrički - St. Andrije Church	K2	1880
Hrvatsko Zagorje	Slani Potok - The Chapel of St. Fabian and St. Sebastian	K4	1880
	Sveti Ivan Zelina - Museum	K2	1880
	Chapel of the Blessed Virgin Mary in Strmec	K4	1880, 1990
	Klanjec – Parish church of the annunciation of the Blessed virgin Mary	K2-K3	1880, 1990
	Gornje Jesenje - The Church of St.John	K3	1880, 1982
	Kraljev Vrh - Three Kings Church	K2	1880, 1990

Conclusion

When it comes to historical and recent earthquakes, what matters from an engineering and societal perspective is the damage and cost, regardless of whether it was caused by a single earthquake or a main/aftershock. From a seismological point of view, even small improvements in the definition of the main seismological parameters of an earthquake that are relevant for a given area (e.g., location of the epicenter, earthquake magnitude) and the definition of local soil conditions are very important. It is of great importance to understand these effects on seismic hazard and risk in order to ensure better mitigation, prevention and reduction of earthquake disasters in the affected stratigraphic and topographic areas.

Acknowledgments

This work was supported by the Croatian Science Foundation under the project “Seismic ground motion amplification induced by topographic irregularity in Northern Croatia” [HRZZ-IP-2022-10-1296].

References

Markušić, S., Stanko, D., Korbar, T., Belić, N., Penava, D., Kordić, B., *The Zagreb (Croatia) M5.5 earthquake on 22 March 2020,* Geosciences, 10 (2020), 7; 252, 21. doi: 10.3390/geosciences10070252

Markušić, S., Stanko, D., Penava, D., Ivančić, I., Bjelotomić Oršulić, O., Korbar, T., Sarhosis, V. *Destructive M6.2 Petrinja Earthquake (Croatia) in 2020—Preliminary Multidisciplinary Research,* Remote sensing, 13 (2021a), 6; 1095, 29. doi: 10.3390/rs13061095

Markušić, S., Stanko, D., Penava, D., Trajber, D., Šalić, R. *Preliminary observations on historical castle Trakošćan (Croatia) performance under recent ML ≥ 5.5 earthquakes,* Geosciences, 11 (2021b), 11; 461, 17. doi: 10.3390/geosciences11110461

ACCOUNTING FOR SITE EFFECTS IN THE ASSESSMENTS OF SUSCEPTIBILITY TO CO-SEISMIC SLOPE FAILURES IN HILLTOP TOWNS OF THE SOUTHERN APENNINES

FLAVIANA FREDELLA [1], VINCENZO DEL GAUDIO [2], NICOLA VENISTI [3], PAOLA CAPONE [4], JANUSZ WASOWSKI [5].

[1] *Dipartimento di Scienze della Terra e Geoambientali, Università degli Studi di Bari "Aldo Moro"– Bari, Italy, flaviana.fredella@uniba.it*

[2] *Dipartimento di Scienze della Terra e Geoambientali, Università degli Studi di Bari "Aldo Moro"– Bari, Italy, vincenzo.delgaudio@uniba.it*

[3] *Dipartimento di Scienze della Terra e Geoambientali, Università degli Studi di Bari "Aldo Moro"– Bari, Italy, nicola.venisti@uniba.it*

[4] *Dipartimento di Scienze della Terra e Geoambientali, Università degli Studi di Bari "Aldo Moro"– Bari, Italy, paola.capone@uniba.it*

[5] *Consiglio Nazionale delle Ricerche – Istituto di Ricerca per la Protezione Idrogeologica – Bari, Italy, j.wasowski@ba.irpi.cnr.it*

Introduction

This study reports some advances in a procedure for a regional scale identification of slopes potentially susceptible to earthquakes-induced landslides. The Daunia Mts. (south-eastern Appennines, Italy) were chosen to test the procedure because of i) the widespread presence of marginally stable slopes consisting of clay-rich flysch materials, ii) the presence of active seismogenic sources in the surrounding areas and iii) the large amount of relevant data made available by ongoing seismic microzonation studies. The tested procedure derives from an approach for a probabilistic estimate of the basic resistance demand expressed through the quantity $(A_c)_x$ (Del Gaudio et al., 2003). This parameter represents the critical acceleration a_c that a slope must have to keep the probability of exceeding a critical threshold x of Newmark displacement D_N within a pre-defined probability (e.g. 10% in 50 years). The calculation of $(A_c)_x$ is based on empirical relations linking D_N to a_c and to Arias Intensity (Arias, 1970), the latter used as a measure of seismic shaking energy.

Methods

In this study we focused on the first step of a three-stage procedure consisting of: i) estimating the resistance demand $(A_c)_x$ placed by local seismicity on the slope; ii) comparing it to the actual slope resistance a_c and iii) classifying slope susceptibility to seismically induced failures, based on differences between $(A_c)_x$ and a_c.

For implementing stage (i), we first updated basic maps of $(A_c)_x$ obtained in previous works for Daunia Mts., using the latest version of tools for seismic hazard assessment and adopting x = 10 cm as critical threshold of D_N for earth slopes. Compared to previous studies, however, we intend to integrate the calculation of the resistance demand by taking into account the site amplification of ground shaking, which can occur on slopes, especially where softer materials overlie a stiffer substratum. For an expeditious estimate of the site amplification, we utilize the ambient noise analysis recordings acquired during the seismic microzonation conducted in Daunia urban and peri-urban areas. Data already processed with a standard method (Nakamura, 1989) are now reanalysed with a more recent technique (HVIP - Del Gaudio, 2017), which provides estimates of the ellipticity of Rayleigh waves as function of frequency. These estimates show peak values of horizontal to vertical ratios of ground motion amplitude (H/V) at resonance frequencies. Such estimates are expected to be more stable and better correlated to the local amplification factor.

At this stage, site effects are incorporated through a simplified calculation of local seismic response, adopting 1D models of site conditions. These models are based on stratigraphies derived from pre-existing boreholes and results of previous geophysical investigations, integrated with purposely

conducted geological surveys and ambient noise data inversion in terms of velocity vertical profiles (Figure 1).

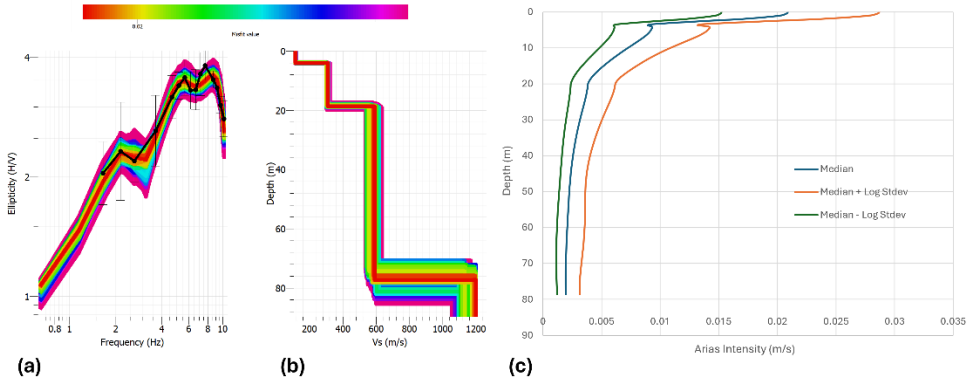

Figure 1. Steps to estimate amplification factors of Arias intensity from 1D site response modelling using ambient noise data: (a) fit between experimental and theoretical curve of Rayleigh wave ellipticity and (b) the corresponding Vs profile obtained using the software DINVER (Wathelet, 2005) for data inversion; (c) Arias intensity vertical profile obtained with the code STRATA (Kottke et al., 2013) to calculate the amplification factor.

Results

The new estimates of $(A_c)_{10}$ resulting from database update give an increase of 50% (from 0.04 to 0.06 g) of their maximum values, which is strongly influenced by the redefined geometry of the seismogenic zones. The first estimates of the site response effect on 16 sites of 3 municipalities show amplification factors in terms of Arias intensity between 3 and 7, which would imply a further increase of the resistance demand in terms of slope critical acceleration by a factor of between 2 and 4.

Conclusion

In view of identifying potential areas of criticalities related to slope destabilization in regional seismic scenarios, the results of the first tests show the importance of incorporating site amplification effects in the calculation of the slope resistance demand placed by the regional seismicity. As next step we intend to evaluate, in estimating the site amplification influence on slope resistance demand, the uncertainties related to the use of simplified 1D models of site condition, by comparing these estimates with the results of 2D/3D modelling. Furthermore, we intend to verify the possibility of extending expeditious estimates of site amplification on slope stability under seismic shaking through empirical relationships providing expected amplification factors, directly based on the results of ambient noise analysis.

References

Arias A. A measure of earthquake intensity, *in Seismic Design for Nuclear Power Plants, R. J. Hansen (ed), MIT Press, Cambridge, Massachusetts.* 1970, 438-483.

Del Gaudio V.; 2017: Instantaneous polarization analysis of ambient noise recordings in site response investigations. *J. Geophys. Int.* 2017. 210, 443-464.

Del Gaudio V.; Pierri P.; Wasowski J. An Approach to Time-Probabilistic Evaluation of Seismically Induced Landslide Hazard. *Bulletin of the Seismological Society of America*. 2003, 93, 2, 557-569.

Kottke R.; Wang X.; Rathje E. Technical Manual for Strata. *Geotechnical Engineering Center*, - *University of Texas*. 2013, 89 pages.

Nakamura Y. A method for dynamic characteristics estimation of subsurface using microtremor on the ground surface. *Q. Report Railway Tech. Res. Inst.* 1994**,** 30, 25-33.

Wathelet, M. Array recordings of ambient vibrations: surface-wave inversion, PhD thesis, Liège University, Belgium. 2005.

ASSESSING THE LIQUEFACTION EJECTA POTENTIAL BASED ON CPTu; CASE STUDY PINIADA VALLEY, GREECE

GEORGE PAPATHANASSIOU [1], LYDIA GOERLOK [1], SOTIRIS VALKANIOTIS [2], MARIA TAFTSOGLOU [2]

[1] *Aristotle University of Thessaloniki, Greece,* gpapatha@geo.auth.gr

[2] *Democritus University of Thrace, Greece*

Introduction

The 2021 Damasi, Greece earthquake Mw=6.3 triggered numerous liquefaction phenomena at the Piniada Valley. The liquefaction features were reported during a field survey conducetd few hours after the event along the Piniada Valley. They were classified as sand craters, as singular features as well as aligned ones, and ground fissures, from where a mixture of water and fine sandy and silty material was ejected, and lateral spreading phenomena. According to eyewitnesses, the phenomena, occurred during the March 3rd mainshock, locally caused mixed fluid fountaining as high as 1 m from the topographic surface. The total area covered by the ejected material (sand blow) at Piniada Valley was estimated as 0.0325 km^2, approximately 0.5% of the zone that is delimited by the village Piniada, to the north, and the present-day river channel of river Pinios, to the south (Papathanassiou et al. 2022).

This area is covered by Holocene sediments deposited along the meandering fluvial system of Pinios. The characteristic evolution of Pinios River dictates the depositional process of the sediments and contributed to the lateral and vertical heterogeneity of the surficial soil material. That was clearly shown during the 2021 event since liquefaction phenomena preferred to concentrate in specific location forming clusters of liquefaction-induced ground disruption such as sand boils, craters and ground fissures. In addition, it is highlighted that within a short distance, the severity of ejecta was totally different. The goal of this study is to investigate the liquefaction potential of a selected area located within a point bar, based on data provided by Cone Penetration Tests with pore water pressure measurement (CPTu).

Methods

On March 2024, a campaign focusing on the conduction of CPTu in selected sites at Piniada valley took place. The goal of this campaign was to investigate the liquefaction potential of a selected area of 400m^2 located within a point bar deposit. Thus, it was decided to perform 6 CPTu up to a depth of 15 meters in an distance of 15 among them ((Fig. 1); 3 on areas of liquefaction manifestations (CPTu1, CPTu2 and CPTu4) and 3 on non-liquefiable sites (CPTu3, CPTu5 and CPTu6).

Figure 2. Locations of CPTu tests. View of ejecta captured by the UAV-campaign conducted few days after the event (Papathanassiou et al. 2022)

Results

The data provided by the in-situ tests were proceed with the Cliq software deveoloped by Geologismiki and the liquefaction Potential Index (LPI) per site was computed. As it is shown in figure 2, the LPI

values of CPTu varies depending the methodogy applied for the computation. In addition, based on the classification suggested by Iwasaki et al. (1978) and the methology proposed by Boulanger and Idriss (2014), the LPI values (>10) of CPTu1, CPTu2, CPTu3 and CPTu4 indicates that surface manifestations should be expected to be triggered by the Damasi 2021 event of M6.3 and of PGA value equal to 0.3g. On the contrary, for the sites where the CPTu5 and CPTu6 were conducted, the liquefaction potential is lower compared to the others sites.

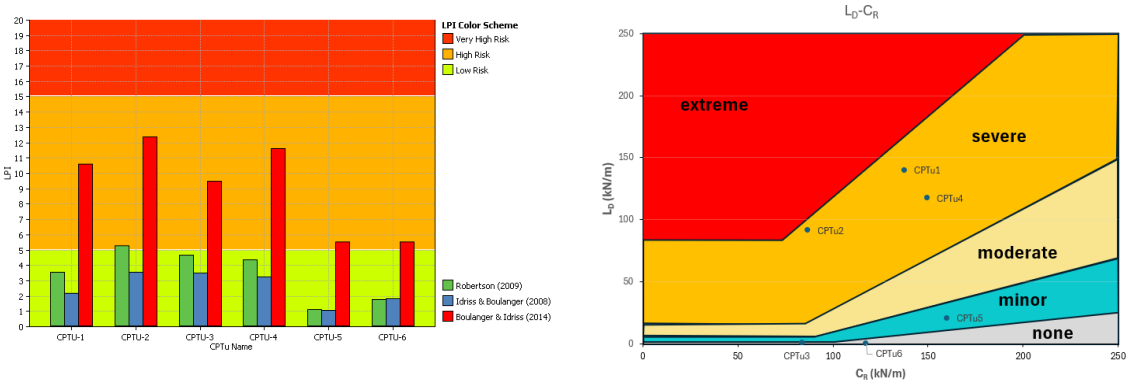

Figure 2. Left. LPI values of CPTu tests. **Right**. CPTu on the diagram of Liquefaction Ejecta Demand (L_D)-Crust Resistance (C_r).

In addition, the liquefaction ejection severity procedure was applied (Hutabarat and Bray 2022) aiming to examine the accuracy of this recently suggested method. The outcome (Fig. 2) is that CPTu1, CPTu 2 and CPTu4 are plotted in the area described as severe ejecta cases, while the CPTu3 and CPTu6 as none ejecta one. The area where the CPTu5 conducted is considered as an area of minor ejecta severity.

Conclusion

Between these two approaches there is mismatch for CPTu3 which was classified as high liquefaction potential area, based on LPI approach, and as a none ejecta case based on the methodology of "ejecta severity". Following the post-earthquake mapping of liquefaction phenomena triggered by Damasi 2021 event (Papathanassiou et al. 2022), the site where the CPTu3 was conducted is classified as a non-liquefaction surface manifestation one. Thus, in this case the ejecta severity approach, recently proposed by Hutabarat and Bray (2022), succesfully predict the real case scenario. On the other hand, the case of CPTu5 was classified as a minor ejecta site which is not in agreement with the results of the conducted survey, where liquefaction phenomena were not reported.

In addition, it could be stated that though the fact that all the area is surficial characterized as point bar deposits, the expected vertical and lateral heterogeneity of the soil stratigraphy could be the main reasons for this differentiation regarding the liquefaction manifetsation even in a distance of few meters.

Acknowledgment

The CPTu campaign was funded by the Research Committee of Aristotle University of Thessaloniki.

References

Hutabarat, D., Bray, J. Estimating the Severity of Liquefaction Ejecta Using the Cone Penetration Test. Journal of Geotechnical and Geoenvironmental Engineering 2022. 148. 04021195. 10.1061/(ASCE)GT.1943-5606.0002744.

Papathanassiou G., Valkaniotis S., Ganas Ath., Stampolidis A., Rapri D., Caputo R., 2022. Floodplain evolution and its influence on liquefaction clustering: the case study of March 2021 Thessaly, Greece, seismic sequence, Engineering Geology, 2022, 298, 106542

Iwasaki, T, Tatsuoka, F., Tokida, K, and Yasuda, S. A Practical Method for Assessing Soil Liquefaction Potential Based on Case Studies at Various Sites in Japan, 2nd International Conference on Microzonation for Safer Construction Research and Application, 1978, 885-896

NATIONAL SCALE EARTHQUAKE SUSCEPTIBILITY MAPPING UTILIZING EXPLAINABLE ARTIFICIAL INTELLIGENCE IN THE NEPAL HIMALAYA

SUCHITA SHRESTHA[1], ANANTA MAN SINGH PRADHAN [2], TAE-SEOB KANG [3]

[1] *Department of Mines and Geology, Ministry of Industry, Commerce and Supplies, Government of Nepal, Lainchour, Kathmandu, Nepal, suchitashrestha@gmail.com*

[2] *Ministry of Energy, Water Resources and Irrigation, Government of Nepal, Nepal, anantageo@hotmail.com*

[3] *Division of Earth Environmental System Science, Pukyong National University, Busan 48513, Republic of Korea, tskang@pknu.ac.kr*

Introduction

Nepal is situated in one of the world's most earthquake-prone areas due to its position in a geologically intricate zone where the Indian tectonic plate meets the Eurasian plate. The continuous convergence of these plates results in frequent seismic activity, with shifts along fault lines often leading to powerful earthquakes in the region. Most of the casualties and damage from past and recent earthquakes in Nepal are due to the country's vulnerable infrastructure (Gautam & Chaulagain, 2016). Nepal is undergoing significant annual population growth, rapid urbanization, and extensive infrastructure development. Unfortunately, this rapid development, often without adherence to earthquake codes, has heightened the region's earthquake risk. The seismic activity observed in recent decades underscores the potential for future earthquakes to impact this densely populated area. This study was focus on enhancing spatial probability mapping using explainable artificial intelligence (XAI). Traditional seismic hazard zone (SHZ) methods typically rely on statistical analyses of historical earthquake data, which can be limited in scope. XAI offers a solution by integrating diverse geological, geomorphological, and geophysical data, thereby expanding the analytical framework. Unlike traditional methods like probabilistic seismic hazard analysis, which often involve complex mathematical models and algorithms, XAI employs machine learning (ML) algorithms designed to generate transparent and interpretable outcomes. This makes it more accessible for scientists, engineers, and policymakers to grasp the underlying factors influencing seismic hazard assessments.

Methods

The earthquake catalog encompasses data from all historical earthquake events within the study area, regardless of their sources, magnitude scales, recording agencies, or event sizes. Geo-related covariates are important in earthquake studies because they can help identify areas that are likely to experience earthquakes. Previous studies on earthquake hazards and probabilities derived several relevant factors for earthquake probability assessments. Elevation (Elv), topographic position index (TPI), magnitude density (MagDen), depth density (DepDen), fault proximity (FaultProx), fault density (FaultDen), and “tectonic zone” covariates are crucial factors that contribute significantly to the assessment of earthquake probability. The rise of AI has been meteoric in recent years, promising transformative changes across various industries. However, the increasing reliance on black-box machine learning (ML) models for critical predictions has raised concerns about the opacity of their decision-making processes. This lack of transparency has sparked a demand among stakeholders for more understandable AI systems (Nguyen et al., 2021). Explainable AI (XAI) aims to address this challenge by developing ML techniques that are not only accurate but also interpretable. When applying XAI techniques alongside modeling approaches such as Random Forest (RF) and Extreme Gradient Boosting (XGB), the objective is to create models that retain high accuracy while providing clear explanations of their reasoning.

Results

We utilized a set of seven geo-related covariates to develop two predictive models: Random Forest (RF) and Extreme Gradient Boosting (XGB). Among these covariates, "tectonic" was a categorical factor.

The values of all seven covariates were numerically encoded in a spreadsheet, with earthquake and non-earthquake cases designated as the target outcomes. Numeric values representing earthquake probability were assigned to distinct datasets. These forecasted values, confined within the 0 to 1 range, can be interpreted as probabilities. Figure 1a illustrates the distribution of earthquake probability values obtained using the RF model, while Figure 1b depicts the earthquake probabilities generated by the XGB model across the Nepalese Himalayas.

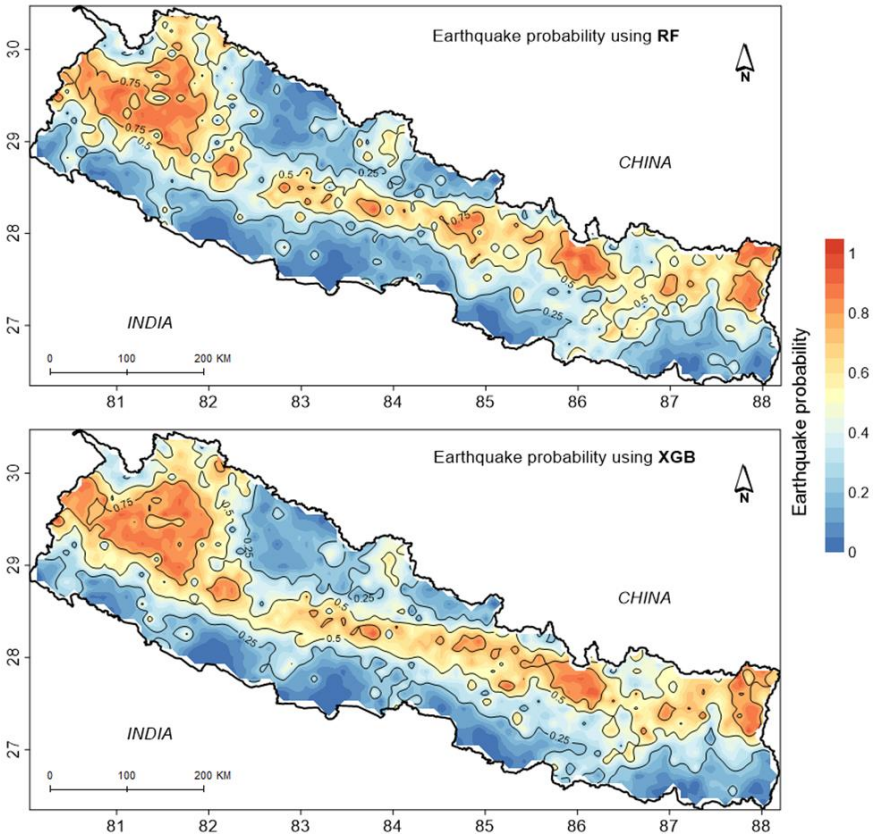

Figure 1. Earthquake probability map of Nepal generated by the a) random forest (RF) and b) extreme gradient boosting (XGB) models.

In the overall process, 1,710 earthquake and non-earthquake instances were analyzed. The RF model accurately classified 801 out of 855 earthquake events and 800 out of 855 non-earthquake events. In comparison, the XGB model correctly identified 765 earthquake events and 741 non-earthquake events. The misclassification indices, determined using a confusion matrix, indicate an uncertainty of 6.37% for the RF model and 11.93% for the XGB model.

Conclusion

The RF model exhibited excellent predictive performance with an AUC of 0.79, while the XGB model demonstrated an AUC of 0.76, indicating a strong goodness-of-fit. For future studies, we recommend exploring the impacts of additional geo-related covariates and incorporating findings from precursor studies to enhance the accuracy of earthquake probability assessments.

References

Gautam, D.; Chaulagain H Structural performance and associated lessons to be learned from world earthquakes in Nepal after 25 April 2015 (MW 7.8) Gorkha earthquake. *Engineering Failure Analysis 68:222–243* (2016).

A GEOLOGICAL AND GEOPHYSICAL INTERPRETATION OF GRAVEL LIQUEFACTION SITE EFFECTS FOLLOWING THE Mw 6.4 PETRINJA (CROATIA) EARTHQUAKE

NIKOLA BELIĆ[1], GIUSEPPE DI GIULIO[2], MAURIZIO VASSALLO[2], SARA AMOROSO[2,3], KYLE ROLLINS[4], GABRIELE TARABUSI[2], LUCA MINARELLI[2], MARKO ŠPELIĆ[1], RADOVAN FILJAK[1], LARA WACHA[1], KOSTA URUMOVIĆ[1], AND TOMISLAV KUREČIĆ[1]

[1] *Croatian Geological Survey, Dept. of Geology, Zagreb, Croatia, nbelic©hgi-cgs.hr*

[2]*INGV Istituto Nazionale di Geofisica e Vulcanologia, Roma, Italy, giuseppe.digiulio@ingv.it*

[3]*Univ. of Chieti-Pescara, Dept. of Engineering and Geology, Pescara, Italy, sara.amoroso@unich.it*

[4]*Brigham Young University, Dept. of Civil and Construction Engineering, Provo UT, USA, rollinsk@byu.edu*

Introduction

In December 2020, the city of Petrinja in Central Croatia was struck by a Mw 6.4 earthquake. Liquefaction, coseismic ruptures, lateral spreading, landslides, and other natural phenomena were found up to 20 km from the earthquake epicenter (Maslač et al 2024; Baize et al. 2022; Pollak et al. 2021). Among more than 170 sand-ejecta occurrences, six sites stand out with gravel as the liquefaction material. This distinction encouraged an international team of scientists and engineers to perform an extensive geotechnical investigation (Amoroso et al. 2023). In this work we bring a geological and geophysical interpretation for Site 2, located in the centre of the investigated area (Fig. 1).

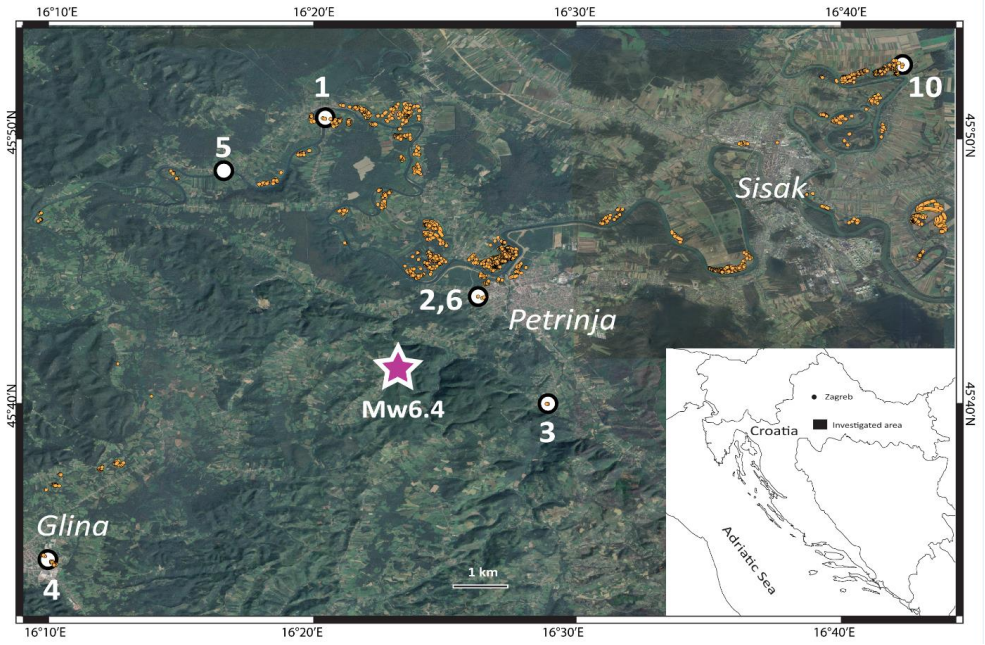

Figure 1. Map of the investigated area: Orange stripes represent liquefaction traces mapped based on the aerial and satellite images (Baize et al. 2022), and the white dots represent the investigated sites.

Methods

Geophysical survey comprised both active and passive investigations. For the active survey (MASW method), we used 48 to 72-point linear arrays of vertical 4.5 Hz geophones, recording 1.5 s signal increments at a sampling rate of 8000 Hz. A 5 kg sledgehammer was used to reproduce forward and reverse shot records to retrieve shear-wave velocity (Vs) profiles (Amoroso et al. 2023; Rollins et al. 2024). For the passive survey (HVSR method), we recorded ambient noise (up to a few hours at each site) using 2D arrays with 20 to 46 seismic nodes, with a sampling rate of 250 Hz. The recordings were

used to compute the surface-wave dispersion curves and horizontal-to-vertical noise spectral ratio (H/V curve), and then to derive site resonance frequencies, important for detecting the presence of seismic contrasts in the subsoil profiles (Di Giulio et al. 2021).

Results

The results from the geophysical surveys were jointly used to perform the inversions and define shear-wave velocity (Vs) profiles (Park et al. 2007). For data processing and interpretation, we used Geopsy software (Wathelet et al. 2020). At most sites we have recorded fundamental resonance frequency (f_0) of 4 Hz and first-order resonance frequency (f_1) of 0.3 Hz. At Site 2, f_0 corresponds to the seismic contrast between layers with modelled share wave velocity (Vs) of 60 and 200 m/s, and f_1 corresponds to the seismic contrast between layers with modelled share wave velocity (Vs) of 200 and 550 m/s (Fig. 2 a). Shear-wave velocity in the first 30 m (Vs_{30}) was calculated at 272 m/s.

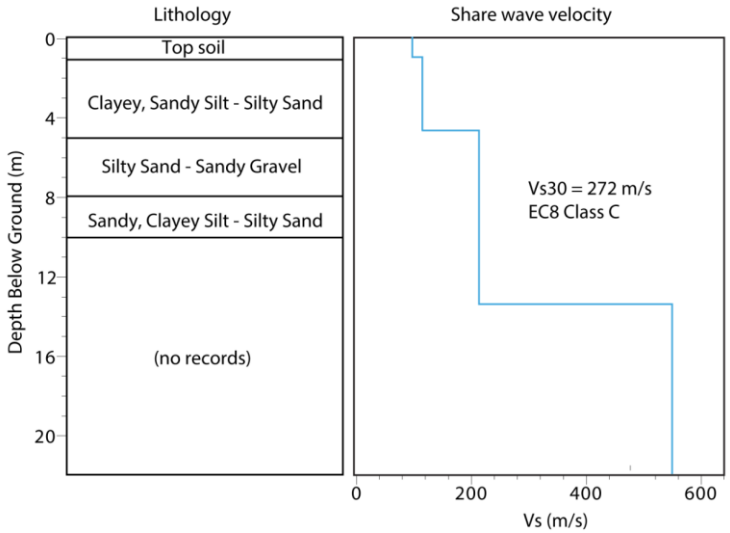

Figure 2. (a) Lithological profile derived from geotechnical borehole at Site 2 (left) in comparison to the Vs30 profile for the 0-20 m interval (right).

Conclusion

Based on the comparison between lithostratigraphic description of geotechnical borehole, and modelled shear-wave velocity (Vs) profiles at Site 2, we conclude that the seismic contrast at the fundamental resonance frequency f_0 corresponds to the lithological boundary between clayey silty sand – sitty sand, and, silty sand – silty gravel, recorded at 5 m in the geotechnical borehole. The bottom layer (5 – 8 m from the surface) is, most probably, the source for the liquefaction material. The seismic contrast at the first order resonance frequency f_1 corresponds to the deeper lithological boundary, which was not reached by geotechnical drilling in 2022. Recorded seismic contrasts can be verified to lithological profiles at the borehole site. Further geophysical measurements, and estimated share wave velocity models can extend the geological interpretation to a larger investigation area.

Acknowledgements

Funding for this work was provided by Progetti di Ricerca Libera INGV 2021 (Istituto Nazionale di Geofisica e Vulcanologia) “Liquefaction Assessment of Gravelly Deposits (LAGD; 9999.816): historical data analyses and in situ testing at Italian trial sites to develop innovative methods”, by the Geotechnical Extreme Events Reconnaissance (GEER) organization, by Brigham Young University (Provo, Utah) and by the University of Ferrara (Ferrara, Italy). This support is gratefully acknowleged; however, the opinions, conclusions, and recommendations in this paper do not necessarily represent those of the sponsors.

References

Amoroso, S., K. M. Rollins, G. Di Giulio, L. Wacha, K. Urumović, D. Faieta, R. Filjak, D. Fontana, S. Lugli and M. Manuel. 2023. Geotechnical and geophysical tests following the 2020 earthquake-induced liquefaction phenomena. In Proceedings of the 2nd Croatian Conference on Earthquake Engineering - 2CroCEE. Zagreb, Croatia. https://doi.org/10.5592/CO/2CroCEE.2023.21

Baize, S., Amoroso, S., Belić, N., Benedetti, L., Boncio, P., Budić, M. Cinti, F.R., Henriquet, M., Jamšek Rupnik, P., Kordić, B., Markušić, S., Minarelli, L., Pantosti, D., Pucci, S., Špelić, M., Testa, A., Valkaniotis, S., Vukovski, M., Atanackov, J., Barbača, J., Bavec, M., Brajkovič, R., Brčić, V., Caciagli, M., Celarc, B., Civico, R., De Martini, P.M., Filjak, R., Iezzi F., Moulin, A., Kurečić, T., Métois, M., Nappi, R., Novak, A., Novak, M., Pace, B., Palenik, D. and Ricci T. 2022. Environmental effects and seismogenic source characterization of the December 2020 earthquake sequence near Petrinja, Croatia. Geophysical Journal International, 230(2): pp. 1394–1418. https://doi.org/10.1093/gji/ggac123

Di Giulio, G., Cultrera, G., Cornou, C., Bard, P.Y. and Al Tfaily, B. 2021. Quality assessment for site characterization at seismic stations. Bulletin of Earthquake Engineering 19(12): 4643-4691. https://doi.org/10.1007/s10518-021-01137-6

Maslač J., Belić, N., Budić, M., Cinti, F.R., Kordić, B., Pantosti, D., Pucci, S., Špelić, M., Amoroso, S., Minarelli, L., Valvano, C. (2024). Earthquake Geology Studies in Croatia: active faults and seismic potential project Map portal, GISCloud, https://app113450.giscloud.com

Park, C. B., Miller, R. D., Xia, J. and Ivanov, J. 2007. Multichannel analysis of surface waves (MASW)- Active and passive methods. The Leading Edge 26: 60-64. https://doi.org/10.1190/1.2431832

Pollak, D., Gulam, V., Novosel, T., Avanić, R., Tomljenović, B., Hećej, N., Terzić, J., Stipčević, J., Bačić, M. and Kurečić, T. 2021. The preliminary inventory of coseismic ground failures related to December 2020 – January 2021 Petrinja earthquake series. Geologia Croatica: Journal of the Croatian Geological Survey and the Croatian Geological Society 74(2): 189-208. https://doi.org/10.4154/gc.2021.08

Rollins, K., Amoroso, S., Walburger, A., di Giulio, G., Belić, N., Urumović, K., Filjak, R., Minarelli, L., Tarabusi, G., Stanko, D., Markušić, S., Marenghi, L., & Vassallo, M. (2024). Liquefaction assessment at gravel sites in Croatia based on V s and DPT blow count. Proceedings of the 7th International Conference on Geotechnical and Geophysical Site Characterization, Barcelona, 18 - 21 June 2024